

ANISOTROPIC THERMAL EXPANSIVITY OF ORIENTED POLYPROPYLENE

S. Abdul Jawad
Physics - Department
University of United Arab Emirates

Abstract:

The thermal expansivity of drawn polypropylene has been studied over the temperature range -60°C to $+10^{\circ}\text{C}$ for different draw ratio samples. A high degree of anisotropic expansivity was found. Perpendicular to the draw direction α_{\perp} reaches $190 \times 10^{-6} \text{ }^{\circ}\text{C}^{-1}$, while parallel to the draw direction α_{\parallel} becomes negative for high draw ratio to reach $-11.5 \times 10^{-6} \text{ }^{\circ}\text{C}^{-1}$ at -50°C .

The negative thermal expansion can be interpreted in terms of the entropic frozen-in stresses, and the positive thermal expansion (α_{\parallel}) is found to be related to a combined contribution of the orientation in the crystalline and amorphous phases as a result of deformation process.

The thermal expansion coefficient (α) was found to be nearly constant for different draw ratio samples, a linear relationship was found between (α) and the mean temperature.

Introduction

In common with other physical properties the thermal expansion behaviour of oriented polymers changes dramatically in the major orientation direction with increasing draw ratio. This contrasts with much smaller changes in the transverse direction. It is well established that many high oriented polymers show a negative coefficient of thermal expansion in the draw direction and a positive coefficient of thermal expansion in the transverse direction (1, 2, 3).

The theoretical attempts were published in order to explain the negative thermal expansion coefficient. Choy et al. (2, 3) proposed that the negative coefficient of thermal expansion is related widely to the presence of tie molecules which produce a contraction at high temperature. However, Orchard et al. (1) in a more recent publication have suggested that it relates to the presence of a frozen in stress, which becomes more effective at high temperature due to the fall in the tensile modulus with increasing temperature.

It was shown that this model could give a satisfactory quantitative explanation of the negative coefficient of thermal expansion of highly oriented polyethylene, and predicts a value for the frozen in stress which agreed well with the shrinkage force observed at high temperature.

In this paper the behaviour of a series of oriented polypropylene samples is described. It will be shown that the theoretical modelling suggested by Orchard et al. (1) is applicable for mostly high oriented polypropylene. However less oriented samples show somewhat different behaviour, although the theoretical modelling is still applicable at a phenomenological level of understanding.

Sample Preparation

The polymer used was polypropylene copolymer, propathane GSE 108, melt flow index 0.8, manufactured by Imperial Chemical Industry Ltd. (ICI). Billets were machined from isotropic rod with nominal diameters which varied from 5 to 12 mm. The billets were then die drawn (4) through a conical die with a 15° semi-angle and a 4 mm diameter exit bore. The die assembly was controlled at a temperature of $110 \pm 1^\circ\text{C}$ while the sample was being drawn. Samples were drawn at a speed of 150 mm/min. which produced draw ratio (λ) between 3.7 and 16 ($\lambda = \text{Initial cross sectional area/Final cross sectional area}$) depending on the nominal diameter of the billet used. All the samples were transparent with the exception of the draw ration 16, material which was opaque white due to the formation of microvoids.

Experimental Techniques

Characterization of Samples

Different experimental techniques were carried out in order to study the structure of drawn material of polypropylene, before accomplishing the measurements of thermal expansion coefficient. A summary of these experimental techniques will be given here, however, a detailed description of such techniques can be found elsewhere (5, 6, 7).

X-Ray Diffraction

Wide angle X-ray scattering (WAXS) patterns were obtained using an Enraf-Noni crystallographic unit with filtered $\text{Cu K}\alpha$ radiation and a flat film camera, using 50 minutes exposure time for 3 mm diameter samples.

Small angle X-ray scattering (SAXS) patterns were obtained using a Franks small angle camera manufactured by Searle Instruments Ltd., attached to a siemens microfocuss X-ray tube. The scattering pattern, was recorded on a film and the long period determined from the pattern using a Jouce. Loeble microdensitometer, using the relation,

$$L = S \lambda / r.$$

where l = lamellar periodicity (\AA)
 λ = the wave length of radiation
 S = specimen to film distance
 t = distance of the reflection from the main beam position on the photographic plate.

Differential Scanning Calorimetry

The melting point and the heat of fusion (ΔH_f) were found using perkin-Elmer D5c-2 differential scanning calorimeter. Two heating rates were used $10^\circ\text{C}/\text{min}$ and $80^\circ\text{C}/\text{min}$.

Density measurements

The density of drawn samples was measured by means of the density bottle technique with a mixture of water and methanol as the fluid. The results were checked using titration technique. Taking the theoretical density of polypropylene crystal as calculated by Natta et al. (8), considering the crystal structure as monoclinic cell, the degree of crystallinity was calculated using the relation,

$$\rho = X \rho_c + (1 - X) \rho_a$$

where ρ = density of the sample.

ρ_c, ρ_a = densities of crystalline phase and amorphous phase respectively.
 For crystalline phase $\rho_c = 0.9360 \text{ g/cc}$ and for amorphous phase $\rho_a = 0.8650 \text{ g/cc}$
 X = degree of crystallinity.

Creep modulus measurements

The one minute isochromal modulus at 1% strain was measured in the temperature range 20°C to -60°C . The modulus was determined from three point bend test with a sample length 15 cm.

In this test the sample is supported horizontally at two points and a load is applied at the centre. Surrounding the sample was a polyurethane foam chamber. This was supplied with cold gas boiled off from a dewar of liquid nitrogen which was passed over a heater coil controlled by an Eurotherm proportional temperature controller. The sample temperature was maintained to an accuracy $\pm 0.5^\circ\text{C}$ over the temperature range $+20^\circ\text{C}$ to -60°C .

Thermal Expansion Measurements

For measurements of thermal expansion coefficient a compression type apparatus was used. A 7 mm long sample in the form of cylinder was placed into thermally

insulated chamber as shown in Fig. 1. 18 cm quartz rod was in contact with the upper surface of the sample while its other end attached to the moving element of a transducer. The D.C. output of the transducer is fed to a 3 digit visual display unit to give direct reading in microns. The output from this unit is passed to the x-y plotter as y-component. The x-component is obtained from the output of the thermocouple located at the side of the specimen, and its output passed to a millivolt supply. The millivolt unit can be ramped at a linear rate between predetermined limits, the measurements were made with a ramp time of 10 minutes over all scale range of 1 mv. Change in temperature is introduced by circulating cold gas round the sample from a liquid nitrogen dewar supply through an electrical heating system. The slope of the X-Y plot was used to determine the thermal expansion coefficient, taking into account the thermal expansion of the quartz rod which supports the sample.

Experimental Results

Characterization of Samples

Table 1 gives the density, long period and the degree of crystallinity calculated from the density measurements.

Table 1: Density, long period and degree of crystallinity (X)

Draw Ratio	Density gm/cc	X %	Long period Å ^o
Isotropic	0.9095	62.6	
3.70	0.9084	61.1	177
10.7	0.9055	57.04	183
13.0	0.9015	51.40	194
16.00	0.8935	40.10	210

Table 2 gives the melting point and the heat of fusion at two different heating rate 10°C/min, and 80°C/min. for isotropic and drawn samples.

Table 2: Melting point and heat of fusion (ΔH) for isotropic and drawn samples of polypropylene

Draw Ratio λ	Heating Rate 10°C/min.		80°C/min.	
	Melting point °C	ΔH Cal./gm	Melting point °C	ΔH cal./gm
Isotropic	159.0	13.31	162.80	15.41
3.7	160.34	14.63	163.70	18.36
10.7	161.44	17.08	164.85	21.12
13	161.84	17.91	166.30	21.24
16.0	162.64	18.57	167.75	23.87

The density of the drawn polypropylene decreases, given in Table 1, with increasing draw ratio. However, the degree of crystallinity is expected to increase rather than to decrease with increasing draw ratio. The observed decrease in density is due to creation of microvoids in the draw samples as a result of drawing process. This has been confirmed from (SAXS) pattern which shows two streaks at the edges of the (SAXS) pattern, the intensity of the two streaks increase with increasing draw ratio. It is well known that such streaks are due to the microvoids in the crystalline regions of drawn polypropylene (9). On other hand, the (SAXS) pattern for low draw ratios samples is poorly defined, with increasing draw ratio a two point pattern starts to appear to be well defined at draw ratio 16. This may attributed to developing a lamellar structure.

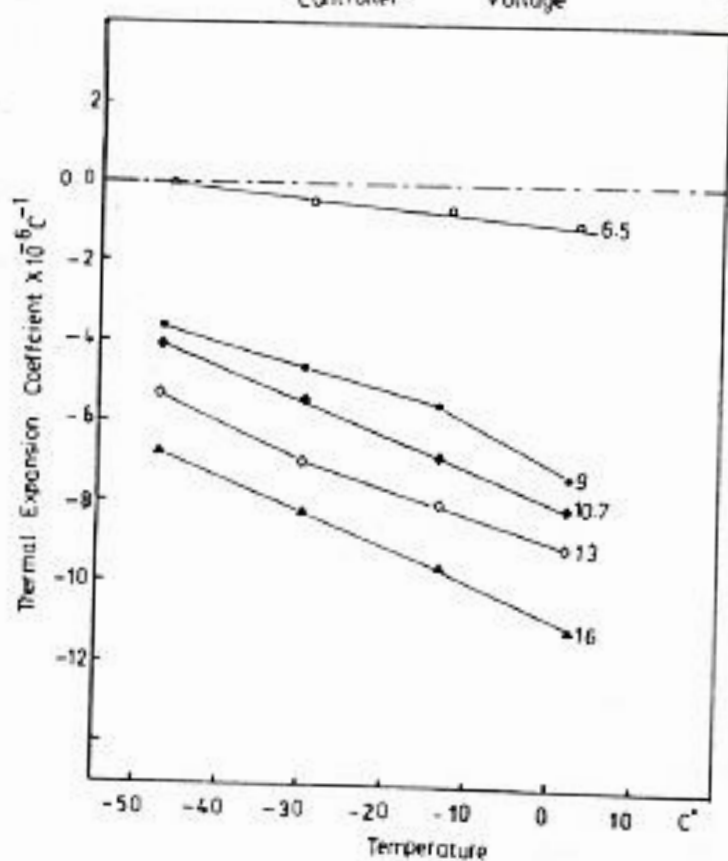
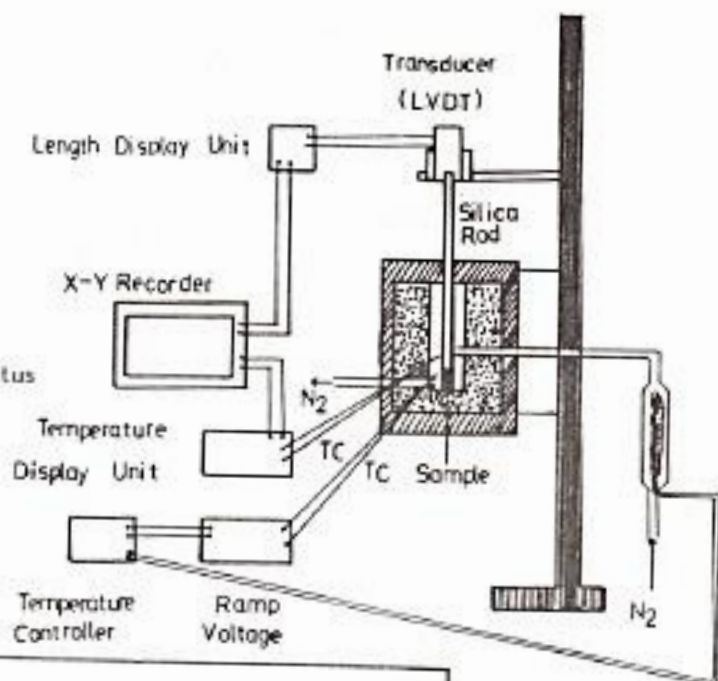
The (WAXS) patterns indicates that most crystalline orientation has occurred during deformations up to a draw ratio 6:1. Large deformations produce only very small increase in orientation.

The melting behaviour of the drawn polypropylene indicates an increase in the melting point from 159°C for isotropic sample to 162.6°C for sample with draw ratio 16, as given in Table 2. This may suggest that the drawing process produced a large crystals and/or smaller surface energy. However, the heat of fusion increases with increasing draw ratio, and this increase is attributed to the increase of crystalline mass fraction upon drawing. It was not possible to calculate the crystalline mass fraction for drawn polypropylene samples since the published data for isotactic polypropylene varies from 15.4 cal./gm to 59 cal./gm, (10-14).

Thermal Expansion Results

The thermal expansion coefficient parallel to the draw direction (α_{\parallel}) is plotted against temperature for the drawn samples of polypropylene as shown in Fig. 2.

Fig.1: Thermal expansion apparatus

Fig.2: Thermal expansion coefficient parallel to the draw direction (θ) versus mean temperature.

A higher values of α_{11}^c were obtained at lower temperature for samples possessing negative thermal expansion, the opposite trend was observed for samples possessing positive thermal expansion as shown in Fig. 3 which shows α_{11}^c against temperature for isotropic sample and draw ratios 3.7 and 2.4.

The thermal expansion coefficient perpendicular to the draw direction α_{\perp} is plotted against temperature as shown in Fig. 4 which shows a decrease in α_{\perp} with decreasing temperature. However, the values for the drawn samples are higher than that for isotropic sample, and α_{\perp} can be considered constant for all drawn samples with a linear relationship with the mean temperature.

If α_{11}^c is plotted as a function of draw ratio as shown in Figure 5, α_{11}^c decrease with draw ratio, from $128 \times 10^{-6} \text{ C}^{-1}$ for isotropic sample to $-11.5 \times 10^{-6} \text{ C}^{-1}$ for draw ratio 16. At mean temperature 2°C becomes 0 at $\lambda = 6$.

Discussion

The structure of the drawn polypropylene can be regarded as crystalline blocks aligned along the draw direction, forming fibrillar stacks of chain folded crystallites, which are connected with crystalline bridges (15). At high draw ratio the structure of the material can be regarded as continuous crystal containing disordered regions which are periodic in the drawn direction.

The observed increase in α_{\perp} upon drawing is mainly due to the crystalline alignment, since the perpendicular thermal expansion of the crystalline phase (α_{\perp}^c) is positive, the contribution of α_{\perp}^c will cause the value of α_{\perp} to increase. Above draw ratio 6 the crystalline component may be regarded as fully oriented. Therefore, α_{\perp} remains nearly constant above draw ratio 6:1. However, α_{11}^c decreases with increasing draw ratio to negative values for sample with $\lambda > 6$.

Choy et al. (2) derived the following relations for the thermal expansion coefficients parallel and perpendicular to the draw direction taking into account the contribution of the amorphous and crystalline phases.

$$\alpha_{\perp} = v\alpha_{\perp}^c + (1-v)\alpha^a + 1/3 \cdot v f_c(\lambda) (\alpha_{\perp}^c - \alpha_{11}^c) \quad (1)$$

$$\alpha_{11} = v\alpha_{11}^c + (1-v)\alpha^a - 1/3 v f_c(\lambda) (\alpha_{\perp}^c - \alpha_{11}^c) \quad (2)$$

where $\alpha^c = 1/3 (\alpha_{\perp}^c + \alpha_{11}^c)$ which is the average expansivity of crystallites.

$f_c(\lambda)$ is the distribution function $= 1/2 (3 \cos^2\theta - 1)$, where θ is the angle between c-axis and the draw direction, α^a is the thermal expansion coefficient of the amorphous phase, v = volume fraction of the crystalline phase,

Fig.3: Thermal expansion coefficient parallel to the draw direction (α_{11}) versus mean temperature for isotropic and low draw ratio.

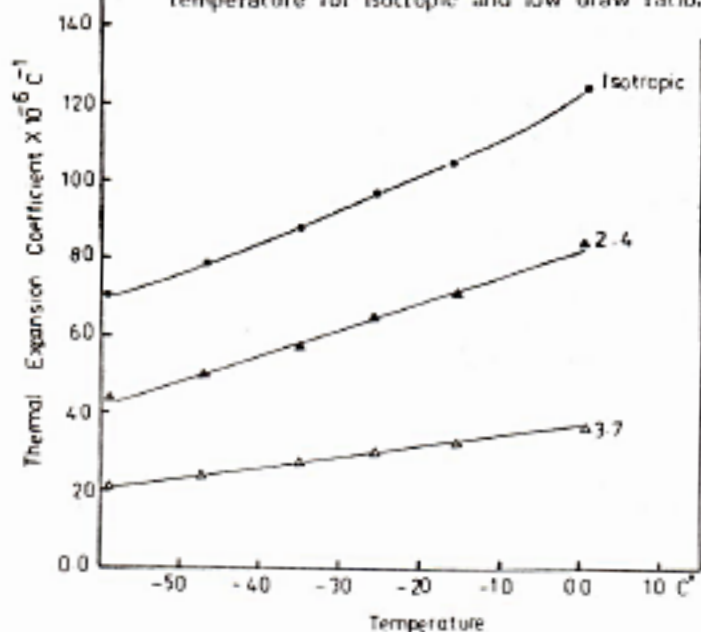
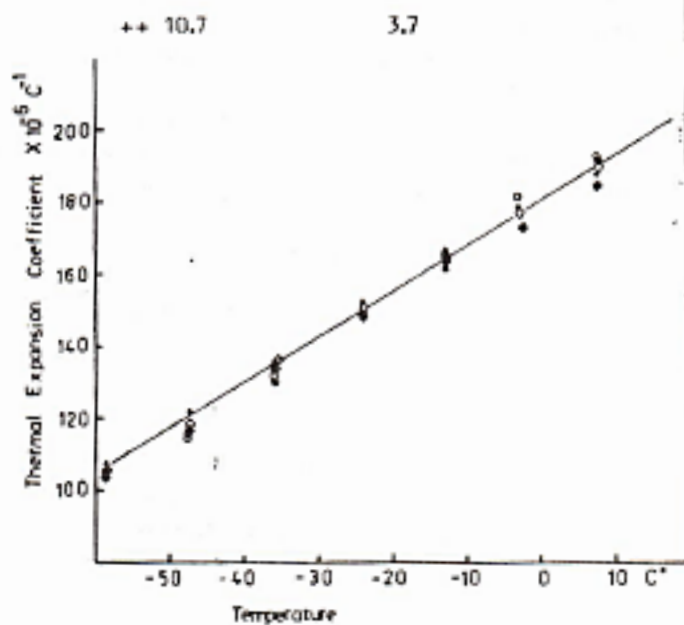


Fig.4: Thermal expansion coefficient perpendicular to the draw direction (α_{\perp}) for drawn samples.



It is well known that the drawn polypropylene achieved the fully orientation state at draw ratio 6:1 (16) which means that $t_c(\lambda) \approx 1$ for a higher draw ratio. This implies that the thermal expansion coefficient for sample with draw ratio > 6 is independent of λ . However, the experimental results show a continuous decrease in α_{11} with increasing draw ratio. On other hand Cepati and Poester (17) derived two other equations for α_{\perp} and α_{11} to take into account the effect of interconnecting crystalline bridge material on the thermal expansion, the derived relations are,

$$\alpha_{\perp} = \alpha_{\perp}^c + \frac{\alpha^a + \alpha_{\perp}^c}{\lambda + 1} \quad (3)$$

$$\text{where } \lambda = \frac{t - t_1}{1 - t} \cdot \frac{E^c}{E_a}$$

$$\alpha_{11} = \alpha_{11}^c + q(\alpha^a - \alpha_{11}^c) \quad (4)$$

$$\text{where } q = \left[(1 - t)^{-1} + t_1 (1 - t_1)^{-1} \frac{E_{11}^c}{E_a} \right]^{-1}$$

Where E_a , E_{\perp}^c , E_{11}^c being the young's modulus of the amorphous regions and the crystalline region perpendicular and parallel to the c-axis, respectively.

t is volume fraction of crystalline region, t_1 is the volume fraction of the interconnecting crystalline bridge material.

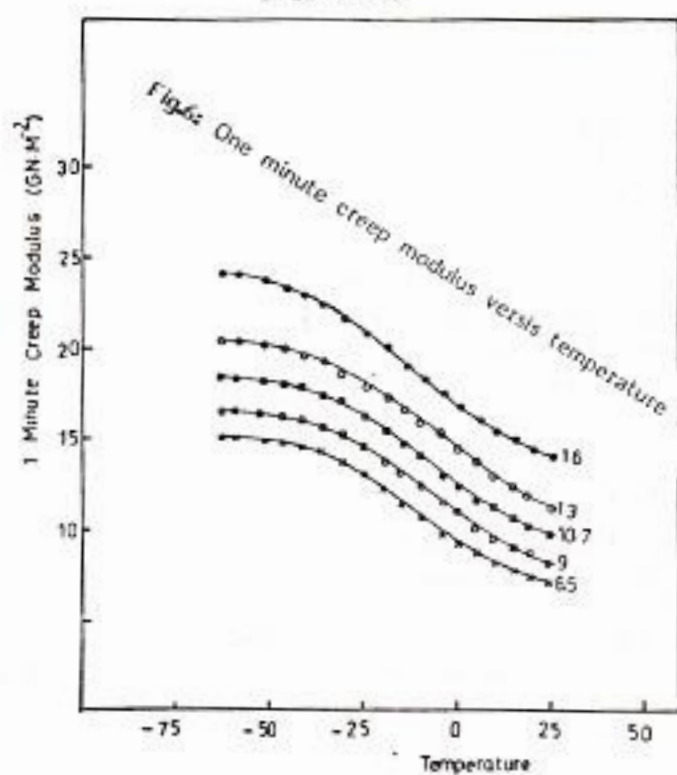
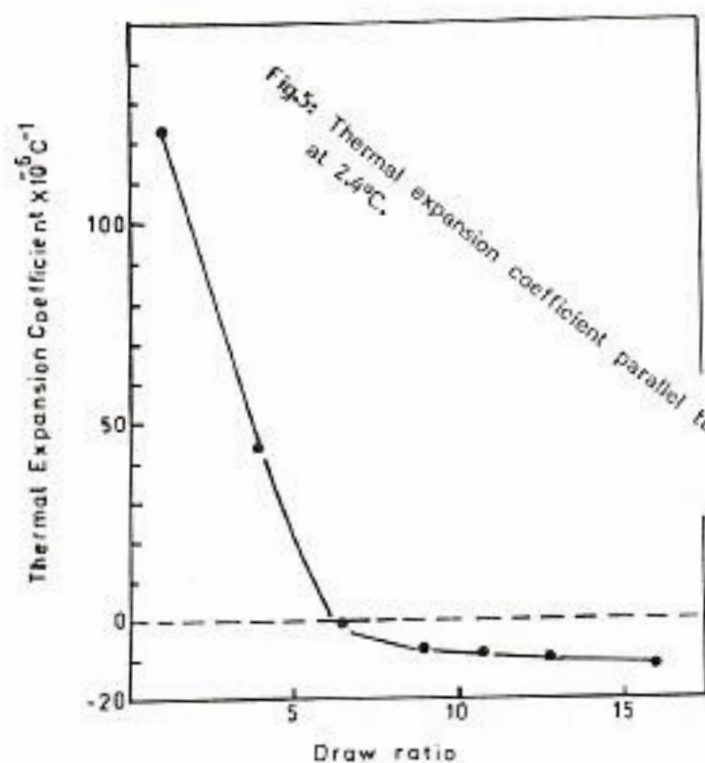
Since $E_{11}^c/E_a \gg 1$, therefore, $q \ll 1$ which means that α_{11} as given in equation 4 is not very strong dependent on λ . This suggest that the strong dependent of the thermal expansion coefficient (α_{11}) on λ is not directly explained in terms of the structural morphology of drawn polypropylene.

In more recent work Orchard et al. (1) suggested that the negative thermal expansion coefficient for highly drawn polyethylene is due to the effect of entropic internal stresses in the amorphous regions, and they related α_{11} to the change in tensile modulus with temperature and the frozen-in stress, the following relation was derived.

$$\alpha_{11} - \alpha_0 = \frac{B}{E} \left(\frac{T}{E} \cdot \frac{dE}{dT} - 1 \right) \quad (5)$$

where α_0 is the intrinsic thermal expansion, and $B = -\sigma/T$ is the shrinkage stress/deg, which depends upon the parameter of the network.

Equation 5 predicts that if the measured thermal expansion α_{11} at various mean temperature are plotted against the corresponding values of $\frac{1}{E} \left(\frac{T}{E} \cdot \frac{dE}{dT} - 1 \right)$, a straight line



will be obtained with a slope B and the value of α_0 at the intercept.

Applying relation 5 to the values of the thermal expansion (α_{11}^c) of the drawn polypropylene samples with one minute creep modulus value for E (Fig. 6), a reasonable linear relationship was found as shown in Fig. 7, which suggests that this theory is applicable for the negative thermal expansion coefficient α_{11}^c of drawn polypropylene. For low draw ratio samples which possess a positive thermal expansion which decreases with decreasing temperature, equation 5 can't be used since the slope of α_{11}^c against temperature is negative, therefore B in equation 5 can't represent the shrinkage stress/deg. as given in this theory. This may suggest that the thermal expansion coefficient for low draw ratios samples is related to the morphology of crystalline and amorphous phases. Therefore we can relate the perpendicular and parallel thermal expansion to the thermal expansion of the amorphous and crystalline phases, and we assume the following relations.

$$\alpha_{11} = a \alpha_{11}^c + b \alpha_{\perp}^c + c \alpha^a \quad (6)$$

$$\alpha_{\perp} = d \alpha_{11}^c + e \alpha_{\perp}^c + f \alpha^a \quad (7)$$

Where a , b , c , d , e , and f are weighting functions related to various structural parameters involving modulus and proportional parts of various components.

Since the temperature dependence of α_{11}^c is very small then,

$$\frac{\delta \alpha_{11}^c}{\delta T} = 0 \quad (8)$$

Therefore, equations 6 and 7 may be written with respect to temperature as follows:

$$\frac{\delta \alpha_{11}}{\delta T} = b \frac{\delta \alpha_{\perp}^c}{\delta T} + c \frac{\delta \alpha^a}{\delta T} \quad (9)$$

$$\text{and } \frac{\delta \alpha_{\perp}}{\delta T} = e \frac{\delta \alpha_{\perp}^c}{\delta T} + f \frac{\delta \alpha^a}{\delta T} \quad (10)$$

The experimental results for α_{\perp} as a function of temperature is very identical for all drawn samples as in Fig. 4. This implies that,

$$\frac{\delta \alpha_{\perp}^c}{\delta T} \propto \frac{\delta \alpha^a}{\delta T} \quad (11)$$

Hence, both the parallel and perpendicular expansivity variations are mainly determined by the perpendicular crystal variability term, so that we may write

$$\frac{\delta \alpha_{11}}{\delta T} = 5 \frac{\delta \alpha_{\perp}}{\delta T} \quad (12)$$

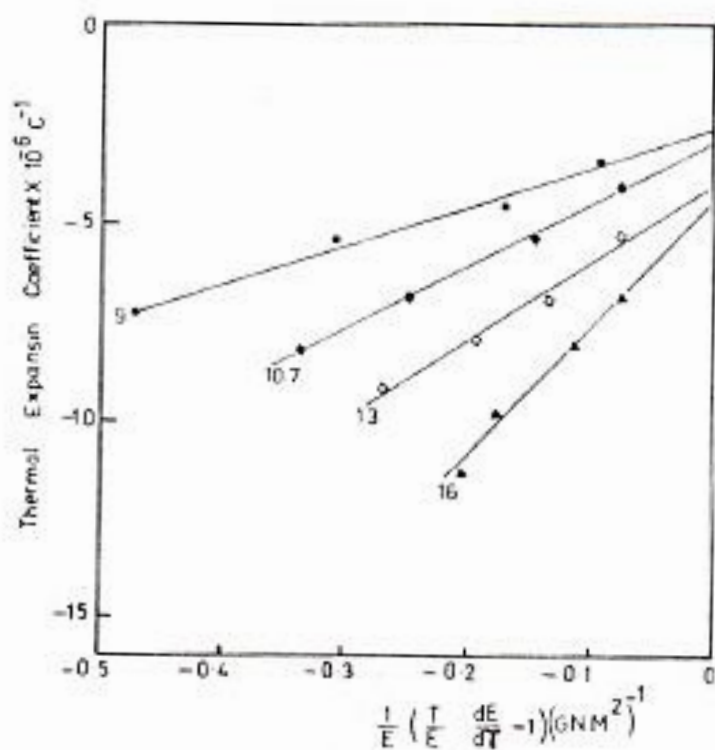


Fig.7: $\frac{1}{E} \left(\frac{T}{E} \cdot \frac{dE}{dT} - 1 \right)$ versus thermal expansion coefficient parallel to the draw direction.

Where S can be considered as a structural factor allowing the combined effects of the crystalline and amorphous contributions in the respective region.

Hence,

$$\alpha_{11}(T_2) = \alpha_{11}(T_1) + S \int_{T_1}^{T_2} \frac{\delta \alpha_{11}(T)}{\delta T} dT \quad (13)$$

However the experimental results for $\alpha_{11}(T)$ against the mean temperature is a straight line as shown in Fig. 4, so that equation 13 may be written in the form,

$$\alpha_{11}(T_2) = \alpha_{11}(T_1) + S \frac{\delta \alpha_{11}(T)}{\delta T} (T_2 - T_1) \quad (14)$$

Where S should be unity for isotropic material, and decreasing with increasing draw ratio.

Equation 14 predicts that if we plot $\alpha_{11}(T_2) - \alpha_{11}(T_1)$ against $(T_2 - T_1)$ a linear relation will be found with a slope equals $S \frac{\delta \alpha_{11}(T)}{\delta T}$. As shown in Figure 3 the relation between $\alpha_{11}(T)$ and mean temperature is nearly a straight line for isotropic and samples with draw ratio 2.4 and 3.7. Taking the slope of α_{11} against temperature the values of S for isotropic is nearly 1 as expected and decreases to 0.61 for draw ratio 2.4 and to 0.26 for draw ratio 3.7. This indicates that the positive values for α_{11} i.e. low draw ratio are due to the contribution of the crystalline and amorphous phases, where the negative thermal expansion α_{11} is due to the entropic frozen-in internal stresses.

References

1. G.A.J. Orchard, G.R. Davies, and I.M. Ward, *Polymer*, Vol. 25, 1203, (1984).
2. C.L. Choy, F.C. Chen, and K.J. Young, *J. Polymer Sci., Polymer Physics Edn.*, Vol. 19, 335, (1981).
3. C.L. Choy, F.C. Chen, and E.L. Ong, *Polymer*, Vol. 20, 1191, (1979).
4. P.D. Coates, and I.M. Ward, *Polymer*, Vol. 20, 1553, (1979).
5. Alexander, L.E., *X-ray Diffraction Methods in Polymer Science*, John-Wiley & Sons, London, (1969).
6. Perlman, P., *General laboratory Technique*, Franklin Publishing Co., Engle-Wood, (1964).
7. Ward, I.M., *Mechanical Properties of Solid Polymers*, John-Wiley & Sons, London (1971).
8. G. Natta, and P. Corradini, *Nuova Cimento Suppl.*, Vol. 15, 40, (1960).
9. A.J. Wills, G. Capaccio, and I.M. Ward, *J. Polymer Sci., Polymer Phys. Edn.*, Vol. 18, 493, (1980).
10. G. Gee, *Proc. Chem. Soc.*, 111, (1957).

11. N.A. Nechitaylo, P.J. Sanin, and I.H. Tolchinski, *Poli. Plast. Massy.*, No. 8, 3, (1965).
12. E. Passaglia, and H.K. Kevorkin, *J. App. Phys.*, Vol. 34, 90, (1963).
13. R.M. Wilkinson, and M. Dole, *J. Polymer Sci., Polymer Phys. Edn.*, Vol. 58, 1089, (1962).
14. I.K. Baum, Z.W. Wilchinsky, and B. Groten, *J. App. Polymer Sci.*, 2723, (1964).
15. A.G. Gibson, G.R. Davies, and I.M. Ward, *Polymer*, Vol. 19, 683, (1978).
16. T. Williams, *J. Materials Sci.*, Vol. 8, 50, (1973).
17. N.J. Capiati, and R.S. Porter, *J. Polymer Sci., Polymer Phys. Edn.*, Vol. 15, 1427, (1977).